LETTERS

Anthropogenic carbon dioxide transport in the Southern Ocean driven by Ekman flow

T. Ito[1], M. Woloszyn[1] & M. Mazloff[2]

The Southern Ocean, with its large surface area and vigorous overturning circulation, is potentially a substantial sink of anthropogenic CO_2 (refs 1–4). Despite its importance, the mechanism and pathways of anthropogenic CO_2 uptake and transport are poorly understood. Regulation of the Southern Ocean carbon sink by the wind-driven Ekman flow, mesoscale eddies and their interaction is under debate[5–8]. Here we use a high-resolution ocean circulation and carbon cycle model to address the mechanisms controlling the Southern Ocean sink of anthropogenic CO_2. The focus of our study is on the intra-annual variability in anthropogenic CO_2 over a two-year time period. We show that the pattern of carbon uptake is correlated with the oceanic vertical exchange. Zonally integrated carbon uptake peaks at the Antarctic polar front. The carbon is then advected away from the uptake regions by the circulation of the Southern Ocean, which is controlled by the interplay among Ekman flow, ocean eddies and subduction of water masses. Although lateral carbon fluxes are locally dominated by the imprint of mesoscale eddies, the Ekman transport is the primary mechanism for the zonally integrated, cross-frontal transport of anthropogenic CO_2. Intra-annual variability of the cross-frontal transport is dominated by the Ekman flow with little compensation from eddies. A budget analysis in the density coordinate highlights the importance of wind-driven transport across the polar front and subduction at the subtropical front. Our results suggest intimate connections between oceanic carbon uptake and climate variability through the temporal variability of Ekman transport.

Previous modelling studies suggest that more than 40% of the uptake of global oceanic anthropogenic CO_2 (ACO_2) occurs in the Southern Ocean[9–11]. In contrast, observational estimates of the ACO_2 inventory are very low; the area south of 50° S holds only 9% of the global oceanic inventory[12]. This apparent difference between the region's significant carbon uptake and minimal storage implies that a large fraction of ACO_2 absorbed into the Southern Ocean is subsequently exported to the northern basins[13]. It is unclear, however, how this transport is achieved. Ocean eddies and jets are dominant features of the Antarctic Circumpolar Current (ACC). Lateral transport by eddy stirring along constant density (isopycnal) surfaces has been hypothesized to explain the northward transport[14]. Although the distribution of some tracers, such as salinity and nutrients, are primarily oriented along isopycnal surfaces, others, such as potential vorticity, have significant gradients across the ACC[15]. The dynamically relevant potential-vorticity gradients across the ACC may inhibit the eddy stirring of tracers at these latitudes, which challenges the hypothesized role of along-isopycnal eddy stirring. Furthermore, isopycnal eddy stirring leads to tracer homogenization, and a northward ACO_2 flux is clearly up-gradient.

The atmosphere overlying the Southern Ocean is undergoing a significant change characterized by a positive trend in the index of the southern annular mode[16,17] and, thus, increasing westerly winds. This climate trend is likely to continue in the coming decades[18]. The Southern Ocean biogeochemistry and associated carbon fluxes will respond to the intensification of meridional overturning circulation driven by the stronger winds[6,7]. Whether the transport driven by the increasing winds will be compensated by an increase in mesoscale-eddy transport is uncertain[8].

Despite its climatic importance, the mechanisms and pathways of ACO_2 transport are poorly understood. Several complications have slowed progress in studying this topic. Horizontal scales of ocean eddies are in the range of 10–100 km and are not explicitly resolved in typical ocean circulation and carbon cycle models. Physical and chemical properties of the Southern Ocean have been historically undersampled owing to its vast area, remoteness and severe weather conditions. Recently, however, supercomputing resources have become available that allow eddy resolutions to be reached. Furthermore, Southern Ocean observations have been greatly increased owing to augmentation of shipboard measurements by satellite sensors and autonomous floats. A high-resolution (1/6° × 1/6° longitude–latitude grid) estimate of the Southern Ocean circulation has been developed by using these resources to make an eddy-permitting ocean general circulation model[19,20] consistent with the modern observations (Methods).

In this study, we couple a marine carbon cycle model to the high-resolution circulation estimate, allowing diagnosis of the physical processes controlling the uptake and lateral transport of ACO_2 in the Southern Ocean. Fluxes and distributions of ACO_2 are determined by comparing two simulations in which the model is forced with the observed atmospheric concentration of CO_2 (contemporary run) and with the constant, pre-industrial CO_2 concentration of 278 parts per million by volume (natural run). The two runs are initialized separately using observational estimates[21] of contemporary and natural carbon in 1995. Then the model is integrated for 12 yr, up to the end of 2006. We focus on the intra-annual variability over the 2-yr period from January 2005 to December 2006. Because this is the first time that such a high-resolution ocean state estimate has been used to study the uptake and transport of ACO_2, we perform extensive model validation to evaluate uncertainties in the simulated ACO_2 distribution (Methods and Supplementary Information). Simulated model fields reproduce the observed pattern of water mass distribution, tracer properties and the seasonal variability of areas covered in sea ice. However, our estimate of anthropogenic carbon is not perfect, and the sources of uncertainty include errors in the initial conditions, simplified parameterization of biological processes and the circulation errors. On the basis of direct comparison with *in situ* observations, the largest discrepancy occurs near the base of the mixed layer and at the fronts, and the standard error in local ACO_2 concentration is less than 16%.

Simulated uptake and column inventory of ACO_2 reveals significant spatial variability and distinct patterns associated with the

[1]Department of Atmospheric Science, Colorado State University, 1371 Campus Delivery, Fort Collins, Colorado 80523-1371, USA. [2]Scripps Institution of Oceanography, University of California, San Diego, 9500 Gilman Drive, La Jolla, California 92093-0230, USA.

ACO$_2$ uptake (mol C m^{-2} yr^{-1})

0   1.0   2.0   3.0   4.0

Column inventory of ACO$_2$ (mol C m^{-2})

0   15   30   45   60
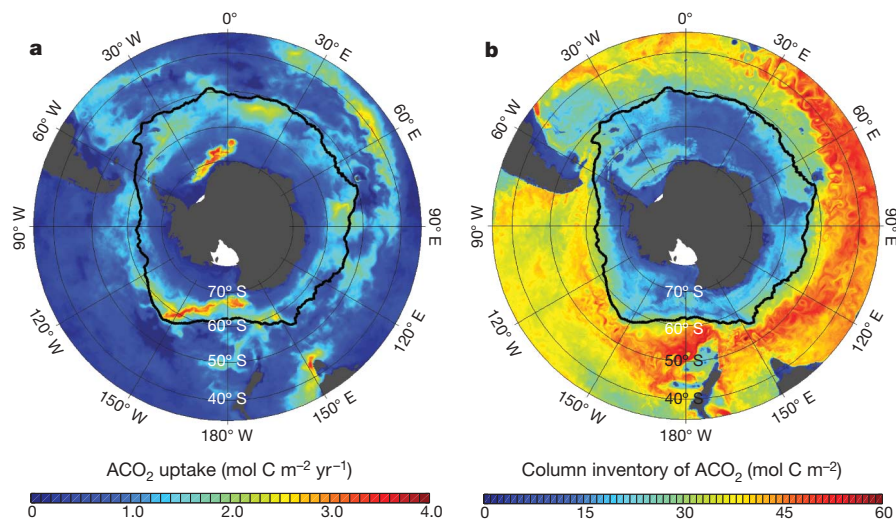
Figure 1 | Uptake and inventory of anthropogenic carbon. a, The 2-yr mean of ACO$_2$ uptake rates evaluated between January 2005 and December 2006; **b,** the column inventory of ACO$_2$ (storage) determined from a 5-d mean in December 2006. The black solid line represents the position of the APF calculated from satellite observations of sea surface temperature[29].

frontal structures of the ACC. Figure 1a highlights the enhanced ACO$_2$ uptake in the three major regions: poleward of the Antarctic polar front (APF), which encircles the globe at ~55° S (marked by the black solid line); the western boundary regions of the subtropical gyres (at the subtropical front at ~40° S); and the high latitudes near the Weddell and Ross seas. These regions are characterized by enhanced oceanic vertical exchange due to convective mixing, wind-driven upwelling and (often topographically induced) mesoscale-eddy variability[22] (Supplementary Information). Spatial correlation (correlation coefficient, $r = 0.51$; significant at the 95% confidence interval) is found between the 2-yr-averaged air–sea ACO$_2$ flux and the logarithm of the standard deviation of vertical velocity at a depth of 225 m. The relatively slow air–sea CO$_2$ exchange (on the order of 1 yr) and the strong lateral advection are probably responsible for the moderate spatial correlation. Other processes (for example air–sea gas exchange rates that depend on the surface wind speed and sea-ice cover) are found to have only minor influences on the uptake. The important role of vertical exchange is consistent with previous studies[5,13] that suggest entrainment of unperturbed deep waters to be the rate-controlling process for the ACO$_2$ uptake.

Figure 1b shows the simulated column inventory of ACO$_2$ in December 2006. The low ACO$_2$ inventory poleward of the APF is in

contrast to the enhanced ACO$_2$ uptake there. The location of the APF separates the polar waters, which are relatively depleted of ACO$_2$, from the relatively enriched sub-Antarctic waters; this is consistent with observational studies indicating low ACO$_2$ storage in the polar regions[12]. The mismatch between the regions of uptake and storage indicates significant up-gradient transport of ACO$_2$ (ref. 13). Mesoscale eddies and meandering jets dominate the local northward transport of ACO$_2$, as is demonstrated by the small scale (10–100-km) alternating transport directions in Fig. 2a. The net northward transport is determined by calculating the zonally averaged ACO$_2$ transports. The northward ACO$_2$ transport is decomposed into the zonal mean and the eddy components, where an eddy is defined as a deviation from a zonal mean. Eddy transport can be further decomposed into transient and stationary components. The zonal mean can be defined in two different ways: along constant-latitude circles and along the mean streamline of the ACC. Although the first definition is simple, using the second removes the effects of the meandering of the mean pathway of the ACC, and the eddy fluxes primarily reflect the mesoscale variability.

Compensations between the mean flow and eddies are crucial in quantifying the lateral carbon transport. Figure 2b shows the decomposition using the zonal mean at constant latitude, where the

Northward transport of ACO$_2$ (mol C m^{-1} s^{-1})

−10   −5   0   +5   +10
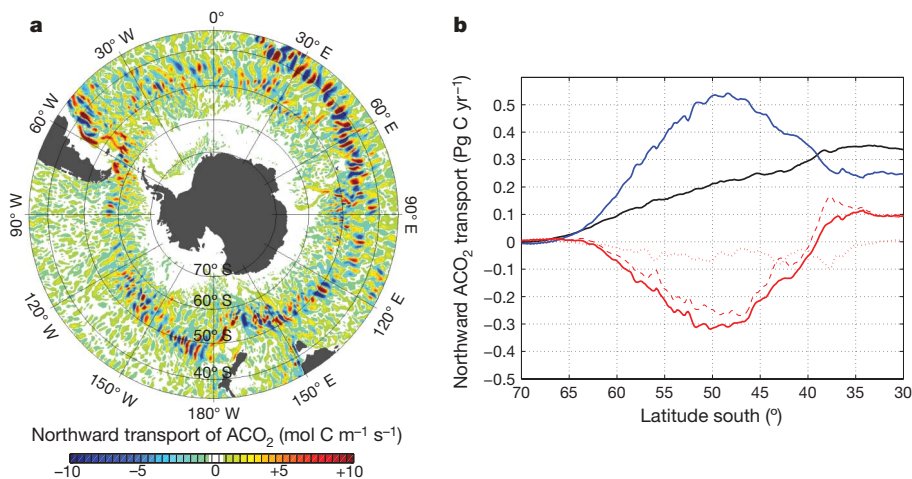
Figure 2 | Northward transport of anthropogenic carbon.
a, Vertically integrated northward ACO$_2$ transport determined from a 5-d mean in December 2006; **b,** the zonally and temporally integrated magnitudes of northward ACO$_2$ flux: zonal-mean (blue), eddy (red) and net

residual (black) transport. Eddy transport is further decomposed into transient (dotted) and stationary (dashed) components. The zonal and temporal mean was calculated along constant-latitude circles for the 2-yr simulation period.
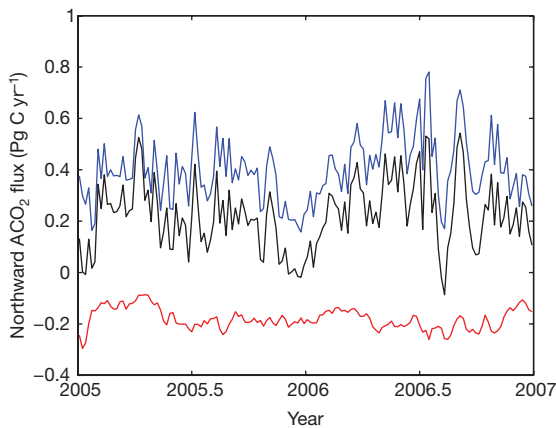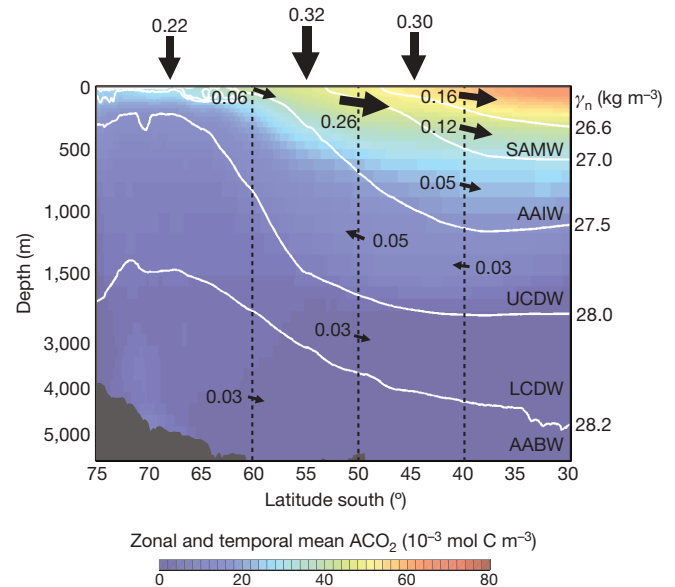
Figure 3 | Variability of anthropogenic carbon transport. Time series of northward cross-frontal ACO_2 flux: zonal-mean (blue), eddy (red) and net (black) transport. The zonal and temporal mean was calculated along the position of the APF for the 2-yr simulation period.

Zonal and temporal mean ACO_2 (10^{-3} mol C m^{-3})

Figure 4 | Vertical structure of anthropogenic carbon transport. Major density layers (differentiated by white lines) are defined using neutral density (γ_n): sub-Antarctic mode water (SAMW), Antarctic intermediate water (AAIW), upper circumpolar deep water (UCDW), lower circumpolar deep water (LCDW) and Antarctic bottom water (AABW). The size of each black arrow is proportional to the magnitude of integrated ACO_2 flux (in units of petagrams of carbon per year); the magnitude is displayed only for fluxes greater than 0.02 Pg C yr^{-1}. Background colour shading indicates zonally and temporally averaged ACO_2. The temporal mean was calculated over the 2-yr simulation period.

net northward ACO_2 transport is achieved by a relatively small residual between a northward mean transport and a southward eddy flux. Eddy transport is primarily dominated by the stationary component. Poleward of 45° S, the mean component results primarily from the strong wind-driven Ekman transport; more than 90% of the mean northward flux occurs in the top 40 m of the ocean at 50° S. Though small-scale eddy fluxes dominate locally, as shown in Fig. 2a, zonally averaged ACO_2 transport is accomplished by means of the zonal-mean circulation.

The main axis of the ACC, as measured by the vertically integrated (barotropic) stream function, is closely aligned with the position of the APF, which is controlled by the topography of the ocean floor. The net cross-frontal ACO_2 transport can then be determined by measuring the zonal mean along the position of the APF, which is essentially identical to the along-streamline mean of the ACO_2 transport. The net northward ACO_2 transport averaged along the APF for the 2-yr simulation period is 0.22 petagrams of carbon (Pg C) per year. Again, this net transport is the residual of a northward zonal-mean transport of 0.41 Pg C yr^{-1} and a southward eddy transport of 0.19 Pg C yr^{-1}. Similar to the zonal mean along constant-latitude circles, the net northward ACO_2 transport involves significant compensation between a northward zonal-mean transport and a southward eddy flux.

The meridional ACO_2 transport shows significant temporal variability (Fig. 3). The standard deviation in the cross-frontal transport is 0.13 Pg C yr^{-1}, and this variability is dominated by the mean component, which explains 90% of the variance of the net transport. The temporal variability of the mean component is almost entirely controlled by the cross-frontal mass flux by Ekman transport (with $r = 0.98$, significant at the 99% confidence interval). Thus, variability in the net cross-frontal ACO_2 transport is essentially driven by the atmospheric wind variability with a decorrelation timescale of about 10 d.

Considering the overall Southern Ocean budget, the spatially integrated oceanic ACO_2 uptake south of 40° S is 0.83 Pg C yr^{-1} over the 2-yr period, which is roughly 40% of the global oceanic ACO_2 uptake[13,23]. Across the latitude circle at 40° S, 0.30 Pg C yr^{-1} (36% of the uptake south of 40° S) is exported to the northern basins. Analysing the vertical structure of the northward ACO_2 transport further illuminates the transport mechanisms (Fig. 4). Although the ACO_2 transport is dominated by the Ekman flow at the latitudes of the APF, the subduction and circulation of thermocline waters become increasingly important northward of the ACC. At 40° S, approximately one-half of the northward ACO_2 transport occurs in the surface layer, probably driven by Ekman dynamics. The other half of the transport occurs below the mixed layer in the density classes of

sub-Antarctic mode water and Antarctic intermediate water, indicating the importance of the dynamics associated with the formation and subduction of these water masses. At 35° S, the northward ACO_2 transport is fairly evenly distributed between the surface and a depth of 600 m, confirming the important role of these water masses in the subtropics.

These results offer new perspectives on our understanding and the quantification of the anthropogenic carbon uptake in the Southern Ocean. The zonal-mean transport, which dominates the net northward transport of ACO_2 across the ACC, is synchronous to the Southern Ocean's zonal wind-stress pattern, indicating a link to atmospheric climate variability. Stronger westerly winds over the Southern Ocean may enhance regional uptake of ACO_2 and increase its transport to the northern basins. It is not yet clear how eddy fluxes may respond to the changes in the westerly wind on interannual and longer timescales. Our analysis demonstrates that there is no compensation on short, intra-annual timescales, over which the variability of northward ACO_2 transport is primarily driven by the variability of wind-driven Ekman transport and is not significantly correlated with that of eddy transport ($r = -0.03$). This raises the question of on what timescales the mean flow–eddy compensation can regulate the cross-frontal fluxes, which is beyond the scope of this paper and is left for future study. Climate variability also affects the natural carbon cycle. It has been suggested that the intensification of surface winds over the Southern Ocean may increase the upwelling of carbon-rich deep waters and the outgassing of natural CO_2 (refs 6, 7). Because the large-scale gradients of anthropogenic and natural CO_2 have opposite signs in the Southern Ocean, opposite sensitivities of anthropogenic and natural carbon fluxes are anticipated. The anthropogenic fraction of atmospheric CO_2 concentration is predicted to increase in the future, and the role of ACO_2 fluxes may become even more important in controlling the total CO_2 uptake. Understanding the mechanisms underlying the uptake and transport of both anthropogenic and natural CO_2, and their interplay, can help in predicting the future oceanic sink of CO_2.

METHODS SUMMARY

We developed a high-resolution ocean circulation and carbon cycle model using an eddy-permitting ocean circulation model with a lateral resolution of $1/6°$. The circulation of the model was optimized to physical observations in a weighted least-squares sense[24,25]. We used a cost function to compare the model to *in situ* observations, altimetric observations and other data sets. Reduction of the model–observation discrepancy was achieved by systematically adjusting the control variables (prescribed atmospheric state and initial conditions) using the adjoint method[26]. We simulated the ocean carbon cycle and air–sea fluxes of CO_2 in offline mode using 5-d-averaged state-estimate fields and a simple biogeochemistry model based on the Ocean Carbon-Cycle Model Intercomparison Project scheme[27], in which biological carbon uptake is parameterized using the linear relaxation of surface phosphate to the monthly mean climatology of the World Ocean Atlas 2005[28]. Anthropogenic components of carbon concentrations and fluxes were determined by subtracting the natural run from the contemporary run. The two runs were initialized in 1995 using two separate initial conditions based on the Global Ocean Data Analysis Project data set[21], which consists of the contemporary and natural components of dissolved inorganic carbon.

Full Methods and any associated references are available in the online version of the paper at www.nature.com/nature.

1. Toggweiler, J. R. & Samuels, B. Effect of Drake Passage on the global thermohaline circulation. *Deep-Sea Res. I* **42**, 477–500 (1995).
2. Sarmiento, J. L. *et al.* Response of ocean ecosystems to climate warming. *Glob. Biogeochem. Cycles* **18**, GB3003 (2004).
3. Russell, J. L., Dixon, K. W., Gnanadesikan, A., Stouffer, R. J. & Toggweiler, J. R. The Southern Hemisphere westerlies in a warming world: propping open the door to the deep ocean. *J. Clim.* **19**, 6382–6390 (2006).
4. Marinov, I., Gnanadesikan, A., Toggweiler, R. & Sarmiento, J. L. The Southern Ocean biogeochemical divide. *Nature* **441**, 964–967 (2006).
5. Ito, T., Marshall, J. & Follows, M. What controls the uptake of transient tracers in the Southern Ocean? *Glob. Biogeochem. Cycles* **18**, GB2021 (2004).
6. Le Quéré, C. *et al.* Saturation of the Southern Ocean CO_2 sink due to recent climate change. *Science* **316**, 1735–1738 (2007).
7. Lovenduski, N. S., Gruber, N. & Doney, S. C. Toward a mechanistic understanding of the decadal trends in the Southern Ocean carbon sink. *Glob. Biogeochem. Cycles* **22**, GB3016 (2008).
8. Böning, C. W., Dispert, A., Visbeck, M., Rintoul, S. R. & Schwarzkopf, F. U. The response of the Antarctic Circumpolar Current to recent climate change. *Nature Geosci.* **1**, 864–869 (2008).
9. Watson, A. J. & Orr, J. C. in *Carbon Dioxide Fluxes in the Global Ocean* (eds Field, J., Fasham, M., Platt, T. & Zeitzschel, B.) 123–141 (Springer, 2003).
10. Orr, J. C. *et al.* Estimates of anthropogenic carbon uptake from four three-dimensional global ocean models. *Glob. Biogeochem. Cycles* **15**, 43–60 (2001).
11. Mikaloff-Fletcher, S. E. *et al.* Inverse estimates of anthropogenic CO_2 uptake, transport, and storage by the ocean. *Glob. Biogeochem. Cycles* **20**, GB2002 (2006).
12. Sabine, C. L. *et al.* The oceanic sink for anthropogenic CO_2. *Science* **305**, 367–371 (2004).
13. Sarmiento, J. L., Orr, J. C. & Siegenthaler, U. A perturbation simulation of CO_2 uptake in an ocean general circulation model. *J. Geophys. Res.* **97**, 3621–3645 (1992).
14. Caldeira, K. & Duffy, P. B. The role of the Southern Ocean in uptake and storage of anthropogenic carbon dioxide. *Science* **287**, 620–622 (2000).
15. Marshall, J., Shuckburgh, E., Jones, H. & Hill, C. Estimates and implications of surface eddy diffusivity in the southern ocean derived from tracer transport. *J. Phys. Oceanogr.* **36**, 1806–1821 (2006).
16. Thompson, D. W. J. & Solomon, S. Interpretation of recent Southern Hemisphere climate change. *Science* **296**, 895–899 (2002).
17. Marshall, G. J. Trends in the southern annular mode from observations and reanalyses. *J. Clim.* **16**, 4134–4143 (2003).
18. Miller, R. L., Schmidt, G. A. & Shindell, D. T. Forced annular variations in the 20th century Intergovernmental Panel on Climate Change Fourth Assessment Report model. *J. Geophys. Res.* **111**, D18101 (2006).
19. Marshall, J., Hill, C., Perelman, L. & Adcroft, A. Hydrostatic, quasi-hydrostatic, and nonhydrostatic ocean modeling. *J. Geophys. Res.* **102**, 5733–5752 (1997).
20. Marshall, J., Adcroft, A., Hill, C., Perelman, L. & Heisey, C. A finite-volume, incompressible Navier Stokes model for studies of the ocean on parallel computers. *J. Geophys. Res.* **102**, 5753–5766 (1997).
21. Key, R. M. *et al.* A global ocean carbon climatology: results from Global Data Analysis Project (GLODAP). *Glob. Biogeochem. Cycles* **18**, GB4031 (2004).
22. Sokolov, S. & Rintoul, S. R. On the relationship between fronts of the Antarctic Circumpolar Current and surface chlorophyll concentrations in the Southern Ocean. *J. Geophys. Res.* **112**, C07030 (2007).
23. Gruber, N. *et al.* Oceanic sources, sinks, and transport of atmospheric CO_2. *Glob. Biogeochem. Cycles* **23**, GB1005 (2009).
24. Mazloff, M. *The Southern Ocean Meridional Overturning Circulation as Diagnosed from an Eddy Permitting State Estimate.* PhD thesis, Massachusetts Inst. Technol. (2008).
25. Mazloff, M. R., Heimbach, P. & Wunsch, C. An eddy permitting Southern Ocean state estimate. *J. Phys. Oceanogr.* (submitted).
26. Wunsch, C. & Heimbach, P. Practical global ocean state estimation. *Physica D* **230**, 197–208 (2007).
27. Najjar, R., Sarmiento, J. & Toggweiler, J. R. Downward transport and fate of organic matter in the ocean: simulations with a general circulation model. *Glob. Biogeochem. Cycles* **6**, 45–76 (1992).
28. Garcia, H. E., Locarnini, R. A., Boyer, T. P. & Antonov, J. I. in *NOAA Atlas NESDIS 64* (ed. Levitus, S.) 396 (US Government Printing Office, 2006).
29. Moore, J. K., Abbott, M. R. & Richman, J. G. Location and dynamics of the Antarctic Polar Front from satellite sea surface temperature data. *J. Geophys. Res.* **104**, 3059–3073 (1999).

Author Contributions T.I. designed and performed numerical simulations of the Southern Ocean carbon cycle and analysed the model output; M.W. performed model–data comparison and calculations of carbon transport; M.M. developed the Southern Ocean State Estimate; all authors contributed to the interpretation of the results and writing of the manuscript.

Author Information Reprints and permissions information is available at www.nature.com/reprints. The authors declare no competing financial interests. Correspondence and requests for materials should be addressed to T.I. (ito@atmos.colostate.edu).

nature

METHODS

Model development. We optimized the Massachusetts Institute of Technology ocean general circulation model[19,20] with a lateral resolution of 1/6°, which obeys the Navier–Stokes equations and conserves mass, heat and salt, to physical observations in a weighted least-squares sense[24,25]. We used a cost function to compare the model output with *in situ* observations (ARGO, CTD, SEaOS, and XBTs), altimetric observations (ENVISAT, GEOSAT, Jason), and other data sets (for example sea surface temperature). Reduction of the model–observation discrepancy was achieved by systematically adjusting the control variables (prescribed atmospheric state and initial conditions) using the adjoint method[26]. Costs associated with control-variable perturbations ensured a physically realistic solution. The Southern Ocean has been very thoroughly observed in the past several years, and the state estimate is now largely consistent with this collection of data[24]. We simulated the ocean carbon cycle and air–sea fluxes of CO_2 in the offline mode using 5-d-averaged state-estimate fields and a simple biogeochemistry scheme[27]. The biogeochemistry model was based on the Ocean Carbon-Cycle Model Intercomparison Project scheme[27], in which biological carbon uptake is parameterized using the linear relaxation of surface phosphate to the monthly mean climatology of the World Ocean Atlas 2005[28]. The model transports five tracers, including dissolved inorganic carbon (DIC), alkalinity, phosphate, dissolved organic phosphate and oxygen. The top 75 m of the modelled phosphate was conditionally restored towards monthly climatology values if the model concentration was greater than that of climatology. Constant stoichiometric ratios were used to calculate the elemental ratio of organic material between phosphate, carbon and oxygen, 1:117:−170, and a constant rain ratio of 0.07 was used to calculate the calcium carbonate formation. One-third of carbon uptake was allocated to the sinking particulate pool, whose vertical dissolution profile is given using a simple power-law function.

We determined anthropogenic components of carbon concentrations and fluxes by subtracting the natural run from the contemporary run. The two runs were initialized in 1995 using two separate initial conditions based on the Global Ocean Data Analysis Project data set[21], which consists of the natural and contemporary components of DIC. Then the model was 'spun up' for 10 yr, to the end of 2004; initial model drifts decreased after a few years of the spin-up integration. We focused on the intra-annual variability over the 2-yr period from January 2005 to December 2006. These calculations required massive computational resources and were made possible by the San Diego Supercomputer Center's DataStar supercomputer and NASA's Columbia and Pleiades supercomputers.

Model validation. We performed extensive model validation to evaluate uncertainties in the simulated ACO_2 distribution. Direct comparison of simulated tracer fields with *in situ* measurements from CLIVAR repeat hydrography lines A16S and P16S demonstrated significant skill in reproducing the observed pattern of water mass distribution and tracer properties. The representations of hydrographic temperature–salinity (T–S) structure and water mass distribution were well reproduced by the model. It is crucial to represent upper-ocean water masses such as SAMW (potential-density range, $26.5\,\mathrm{kg\,m^{-3}} < \sigma_0 < 27.1\,\mathrm{kg\,m^{-3}}$) to reproduce transient tracers such as anthropogenic CO_2 and chlorofluorocarbons. Close examination of the observed T–S profiles showed somewhat tighter gradients in T–S space, suggesting that the model may be overemphasizing the degree of diffusion and mixing. The model–data discrepancy in the *in situ* ocean temperature and salinity was quite small over most of the Southern Ocean. Model–data comparison of biogeochemical tracers such as DIC and alkalinity ensured that the model captured the magnitude and gradients of observed *in situ* distributions; however, these tracers showed a model–data discrepancy greater than that of temperature and salinity. The sources of uncertainty include errors in the initial conditions, simplified parameterization of biological processes, and circulation errors including front position and turbulent tracer mixing.

Errors in DIC and alkalinity can produce errors in the buffer factor and the estimates of anthropogenic carbon. The model was initialized using the Global Ocean Data Analysis Project data set[21] representing the observationally determined three-dimensional distribution of anthropogenic CO_2, and its inventory. The error associated with this initial condition was relatively small; the inventory error was on the order of 7% and the local concentration error was on the order of 20% (ref. 30). Simplified parameterization of biological carbon uptake forces the surface nutrients to remain close to the climatological levels, which may underestimate the variability of biological carbon sources and sinks. Comparison with *in situ* measurements from CLIVAR lines A16S and P16S indicate that the root-mean-squared model–data discrepancies for DIC and alkalinity are respectively 17.8 μM and 17.4 μequiv. $\mathrm{kg^{-1}}$ at the surface layer, and that the discrepancies decrease in the interior ocean. These tracers control the buffer (Revelle) factor, regulating the ability of the sea water to absorb anthropogenic carbon from the atmosphere. Incomplete representation of DIC and alkalinity affects the simulated anthropogenic carbon fluxes through errors in the buffer factor. We estimated the magnitude of this uncertainty to be less than 16%, on the basis of carbonate chemistry calculations.

30. Matsumoto, K. & Gruber, N. How accurate is the estimation of anthropogenic carbon in the ocean? An evaluation of the Delta C* method. *Glob. Biogeochem. Cycles* **19**, GB3014 (2005).